Application of Taguchi Design for Optimization of Corrosion Behavior of Amorphous Silica Thin Film Deposited Through Sol-Gel Dipping Technique

Hamideh Aghasi [1], Sanaz Naghibi [2,*]

[1] Graduated M.Sc. student, Department of Materials Engineering, Shahreza Branch, Islamic Azad University, P.O. Box: 86145-311, Shahreza, Iran.
[2] Assistant professor, Department of Materials Engineering, Shahreza Branch, Islamic Azad University, P.O. Box: 86145-311, Shahreza, Iran.

ARTICLE INFO

Article history:

Received 13 February 2017
Accepted 22 August 2017
Available online 15 December 2017

Keywords:

Amorphous silica
Sol-gel dipping technique
Taguchi approach
Anticorrosion coating

ABSTRACT

Amorphous silica thin films were applied on the 316L stainless steel substrates by sol-gel dipping technique. The starting materials (TEOS, ethanol, HCl, PEG, and NaOH) were used to prepare a gel and then deposited on a substrate. Microstructure, topography, corrosion behavior, and surface hardness were investigated using SEM, AFM, electrochemical method, and micro-hardness measurements. The fabrication parameters utilized to enhance anticorrosion and mechanical properties including calcinations temperature, pH value, and mole ratio of alkoxide to alcohol were studied. Taguchi approach was used as a statistical experimental design technique to set the optimal parameters. Roughness and current corrosion density were evaluated as the response parameter. The pH value is the parameter of the most major effect on the roughness; pH less than or equal to 4 increases the roughness but more pH value decreases the roughness. The ratio of alkoxide to alcohol is the most influential variable on current corrosion density. The increase of alkoxide amount improves the corrosion behavior, which might be related to the increase of the coating density. Consequently, the optimized conditions obtained through Taguchi method target at reaching the highest anticorrosion efficiency involving calcination at 300 °C, pH=6, and the mole ratio of alkoxide to alcohol as 0.167.

1-Introduction

Utilizing ceramic coatings is often related to their properties and structures. Applying these materials on the steel surface improves some characteristics. Such improvement is heavily dependent upon the kind of coating and the method of film preparation. The most outstanding characteristics of these coatings include improving the physical, chemical, and mechanical properties, and promoting resistance against corrosion, chemical attacks, and thermal tensions, without appearance changing. Therefore, the steel lifetime which is nowadays the target of attention of industries will increase. Generally, the coatings are used for manufacturing metal pipes, refrigerators, ovens, repositories, silos, heat exchangers, and the parts exposing to corrosive environments [1-4].

* Corresponding author:
E-mail address: naghibi@iaush.ac.ir

Various methods are applicable for synthesizing ceramic materials which generally require high temperatures. The sol-gel method is popularized due to low heat treatment temperature and convenience in controlling the process to synthesize materials in the form of powder and thin film [5, 6]. SiO_2 is one of the materials that can be applied as an insulating film in electronics by forming a strong physical barrier preventing electron transfer [7]. Silica thin film can be produced using the sol-gel method with a thickness in the range of nanometer to micron [8].

The properties of silica and the merits of sol-gel method justify the extent of studies about sol-gel preparing process of silica thin film.
Gongur et al. investigated the sol-gel process of silica coating on the stainless steel. Using mechanical vibration during the dipping process led to the increase of the thickness of the as-prepared film and the improvement of corrosion resistance. [4].

Yogesh et al. demonstrated that using the polymeric materials such as tri-methyl chlorosilane and hexane as the surface modification agents in the sol-gel process causes the formation of a hydrophobic silica xerogel thin film, increasing the corrosion resistance of the substrate [5].

Gonduz et al. prepared various sols with different combinations adopted from the precursor in the sol-gel silica process. They concluded that any increase in the solvent amount (ethanol) facilitated the crack formation through the solvent emission; therefore, the amount of cracks in the coating would increase after calcinations and, consequently, the coating stability and corrosion resistance would be reduced [9].

Chou et al. used the sol-gel dipping process to form silica thin film over the steel sample. The appropriate calcination temperate was reported to be 300 °C to reduce the amount of cracks. They also noticed that the more the increase of temperature, the more the amount of cracks and this led to the formation of some inappropriate and undesirable combinations such as chromium oxide on the surface [10].

Lopez et al. examined the addition of polymeric components in the sol-gel process of silica coating. They concluded that the addition of methacryloxy propyl trimethoxy silane (MPTMS), hydroxyl methacrylate (HEMA), and trimethoxy methyl silane (MTES) enhanced the corrosion resistance of the coating [11].

Hourmard et al. studied sol-gel silica coating over 316 and 409 steels. They utilized HCl and HF as the catalyst and juxtaposed their behaviors. They reported that applying stronger acids reduced the time of gelling and caused to create a coating with less thickness on the surface [12].

Two research teams studied the influential physical and chemical factors in sol-gel processing of silica and reported that the amount of utilized acid as the catalyst in the hydrolysis process had the greatest effect on the quality of the coating. In this respect, if the mole ratio of water to alkoxide is constant, the density of the dried film will be enhanced by HCl increasing. Additionally, they also found that any increase in water amount leads to improve the porosities and specific surface area of the dried gel [13].

According to the previous researches, it is clear that this coating has positive effects on the surface of steel. Optimization of this process can be considered as a time-consuming procedure due to the number of influential parameters and it seems that there have not been performed any systematic studies in this field. Therefore, applying innovative statistical methods can yield critical results in this system. Utilizing statistical methods in the field of materials science is regarded as a significant issue confirmed and accepted by scientific and industrial societies. In this respect, there have been various researches in various scopes to optimize the synthesis conditions and properties of ceramic materials. A brief survey of the recent studies is provided aiming to the hydrothermal synthesis of titania [14], sialon synthesis via mechanical activation and nitridation process [15], cerium nano-oxide coating on AA7020-T6 alloy [16], application of TiO_2 coating on the surface of titania based on plasma electrolytic oxidation [17], and ZnO coating on the glass surface via the spin coating technique [18].

There exist a number of investigations in the field of ceramic coating optimization. Naghibi et al. prepared a titania thin film on a steel substrate based on the sol-gel method to increase the corrosion resistance and considered the calcination temperature, pH value, PEG amount, and the number of dipping cycles as Taguchi variables. They used L9 orthogonal array to determine the most influential parameter and coating process optimization. After considering the whole circumstances of

the samples, they reported that the amount of PEG, calcination temperature, the number of dipping cycles, and consequently the pH value had the most effects on surface roughness and corrosion resistance, respectively [19].

Despite the presence of various methods for optimizing the processes and their designs, Taguchi method is the only one in which each factor is utilized in independent levels and it diminishes the overall time of process and the number of experiments. The standard experimental design method based on Taguchi approach causes to form repeatable and stable results, which is rarely observed in other statistical methods [20].

The present research inspects the effect of pH value, the mole ratio of alkoxide to alcohol, and the calcination temperature over the morphology, topography and corrosion behavior of the as-prepared amorphous silica coating on the steel substrates, using the Taguchi method. In this regard, SiO_2 thin film was deposited on the steel bar and the aim is defined as improving the corrosion resistance.

2-Experimental Procedure

2-1-SiO_2 thin film preparation

The starting chemicals were tetra-ethyl orthosilicate (TEOS), ethanol, hydrochloric acid (HCl), polyethylene glycol (PEG), and sodium hydroxide (NaOH). All of them were purchased from Merck and used without further purification.

According to the previous researches, parameters such as pH, the calcination temperature, and the mole ratio of alkoxide to ethanol affect the quality of the formed coated surface. In order to inspect the role of the above-mentioned parameters in the properties of the as-synthesized coated samples, Taguchi statistical method has been utilized. Therefore, each parameter was designed based on Taguchi L9 array, and the experimental conditions were defined in accordance with the previous studies [7, 9]. In this regard, Tables 1 and 2 illustrate the levels of each variable and the experimental design conditions.

The experimental samples made of 316L steel with the dimensions of 10*10*2 (mm^3) were prepared and polished by sandpaper 2000. Then the ultrasonic operation was carried out by using industrial ethanol, industrial acetone, and then distilled water according to the environmental temperature for 10 min, respectively.

The sols were prepared in accordance with Table 2. TEOS was solved in water and then ethanol was added to the solution and stirred for 30 min. An adequate amount of PEG was poured into the solution to reach the concentration of 10 g/L. To provide the hydrolysis condition, pH was adjusted to 1.5 by addition of HCl (0.5 normal) and stirred for 24 h. To increase the pH of the solution to the value reported in Table 2, adequate amounts of NaOH (0.5 normal) were dropped to the solutions and stirred for 24 h.

Table 1. The influential variables over the process and surfaces of each sample.

Variable	Level 1	Level 2	Level 3
pH of the Sol	2	4	6
Molar Ratio of Alkoxide to Ethanol	0.250	0.167	0.125
Calcination Temperature (ºC)	200	300	400

Table 2. The experimental condition, influential variables, and their levels based on L9 Taguchi array

Sample	pH of the Sol	Molar Ratio of Alkoxide to Ethanol	Calcination Temperature (ºC)
1	2	0.250	200
2	2	0.167	300
3	2	0.125	400
4	4	0.250	300
5	4	0.167	400
6	4	0.125	200
7	6	0.250	400
8	6	0.167	200
9	6	0.125	300

The as-prepared sols were applied on the substrates using sol-gel dip coating route at a withdrawal speed of 1.7 mm/s with three cycles of dipping by a dip coater machine (109C, Pasargad Nano Equipment, Tehran, Iran). The coated samples were kept in the open air for half an hour and then kept for 30 min at 70 °C. The drying operation was performed in such a way that no crack or dissociations would be formed. The calcination operation was performed in an electric furnace (Exciton, Iran). The samples were heated to reach the maximum temperature (presented in Table 2) and fixed for 1 h. The heating rate of the furnace was 5 °C/min. Then, it was switched off and cooled down to room temperature.

2-2-Characterization

Phase analysis was carried out by using an X-ray diffractometer (PW3040 Philips Co., Netherland). Phase identification was performed via the utilization of X'pert high score plus software.

Corrosion behavior of the samples was studied via Tafel polarization method using a potentiostat device (Parstat 2273, Princeton Applied Research, USA) in 3 wt. % NaCl solution. The tested cell included 3 electrodes, the prepared sample as a working electrode, a platinum auxiliary electrode, and a saturated Calomel electrode. In this respect, Tafel parameters such as I_{corr}, E_{corr}, EP (corrosion protection efficiency), and the values of anodic and cathodic Tafel constant (βa and βc) were calculated through Powersuit software.

The surface quality of the formed sample was inspected using scanning electron microscopy (FE-SEM, Hitachi S-4160, Japan) and the surface topography and roughness were determined by atomic force microscopy (AFM, DS-95-50E, DME). To measure and compare surface roughness and the topography of the samples, this research determined surface roughness average (Ra: the arithmetic mean of the absolute value of the coordinate roughness), the average root of roughness mean (Rq: mean square surface roughness), the average roughness depth (Rz: the average value of the roughness depths only through successive sampling length), the average square of the surface roughness through the ratio of Rz/Ra, the Kurtosis roughness (R_{Ku}: roughness range), and the Skewness roughness (R_{Sk}: roughness in terms of heights and depths symmetry across the entire surface) through Image Plus software. To calculate the average hardness of the coating samples, we utilized Vickers micro-hardness measurement device. Micro-hardness measurement was carried out according to the ASTM E384-12 standard by using a diamond pyramid probe tip with the imported force of 10 GRF.

3-Results and Discussion

3-1-XRD phase analysis

Silica polymorphic transformation unlike its phase conversion is reversible and diffusion less. In this research, the quartz phase is stable owing to the considered temperature range. The quartz phase has α and β shapes which are stable at high and low temperatures, respectively.

Generally, the conversion of α to β shapes takes place at the temperature range of 550 and 575 °C. Obviously, the amorphous silica phase will not be exposed to polymorphic transformation, since the unavoidable conversion of all silica shapes is specialized for crystalline phases [8]. Fig. 1 illustrates the XRD pattern of the powder sample (Sample 1 was shown as a typical pattern. All the patterns were similar). Phase inspection shows that the diffraction pattern is similar for all samples, illustrating the presence of amorphous silica and the absence of crystalline phases. According to the feasible temperature of stainless steels, the volume changes which take place at the time of phase changes cause to form cracks on the coated samples and weaken the thin film stability [8, 10].

3-2-Microstructural study

Fig. 2 displays FE-SEM images of the samples at magnifications of 60.000 and 150. Compaction and uniformity of the coatings are observable in the images with high magnification. These images also show that the drying operation and heat treatment were carried out acceptably and the departure of organic materials out of the system did not cause to form any cracks. Ceramic nanoparticles incline to be agglomerated in aquatic environment, preventing appropriate distribution of the particles and forming uniform coating over the surface [8].Consequently, it reduces the applicability of the performed coating and the protection property and forms cracks in the coating surface. Utilizing polymeric materials can prevent the formation of nanoparticle aggregates over the surface.

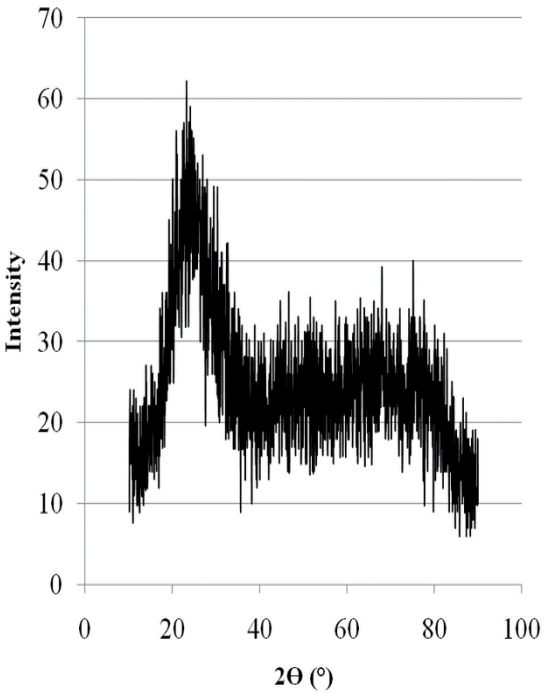

Fig. 1. XRD patterns of the powder of sample 1.

The prevalent polymeric material is PEG for modifying ceramic nanoparticles used for surface modification of titania nanoparticles [14]. A water-soluble polymer such as PEG includes hydroxyl groups at the end of the glycol chains. Since ether oxygen of PEG can be considered as an electron donor for electropositive species (such as hydrogen and metallic atoms), PEG can be absorbed by oligomers. Therefore, PEG forms ligand ring (chelation) and keeps these ions separated from one another by creating steric hindrance. In other words, PEG is regarded as a non-ionized superficial activated factor, which is neutral towards soluble salts and ionized combinations forming the steric hindrance [14]. The steric hindrance generated by the PEG polymer leads to the reduced binding association between particles that results from PEGylation. An overall improved uniformity of particles distribution can be interpreted not only to improve coating homogeneity but also to consolidate the conjugation of the thin film to the substrate. In addition to the steric hindrance effect of PEG, further effects also arise during the drying of the as-deposited thin films. The drying shrinkage is the main cause of cracks formation and propagation. The PEGylation leads to improve the green strength of the coatings and hinder crack expansion. According to these images, one can claim that the utilized coating method in this research can be effective to yield appropriate coatings.

The calculated values of roughness parameters are provided in Table 3.As can be seen, the highest amount of roughness is observed in samples 4 and 3, (24.6 and 22.5 nm), while the lowest amount of roughness is observed in samples 8 and 9 (3.3 nm). Therefore, it is clear that the increase of pH up to 6 reduces the roughness. To determine the increase of roughness for samples 3 and 4, it is necessary to use statistical analysis, as shall be elaborated in the following.

The consideration of the roughness parameter for samples 1, 2, and 3 with similar pH values (pH=2) reveals that the surface roughness is increased by an increase in the ethanol amount and calcination temperature. However, this trend is completely different from the second (samples 4, 5, and 6) and the third series (samples 7, 8, and 9) of the samples. This signifies that when pH equals 4 and also 6, the increase of ethanol and temperature causes to reduce first and then increase the roughness. To verify this issue, the isoelectric point should be considered. This circumstance takes place in pH=2 [8] and signifies the fact that the surface of SiO_2 particles is uncharged at the mentioned pH in the sol-gel process. In this situation, decreasing the alkoxide to ethanol ratio increases the intervals among crystallites due to the low concentration of the Si-alkoxide; therefore, highly appropriate growth conditions of the particles are prepared. On the other hand, solution viscosity due to alcohol increases as the solvent reduces and affects the process of coating. Thus, the formed particles with more intervals and bigger sizes are formed over the substrate surface, leading to the increase in the roughness of the first series of the samples.

pH accretion to a greater values makes the surface of particles to be charged and this creates repulsion among the crystals. This repulsion causes to form smaller particles with fewer intervals and correspondingly reduces the surface roughness.

The surface roughness changing trend in the second (samples 4, 5, and 6) and third (samples 7, 8, and 9) series of the samples is different from that of the first series (samples 1, 2, and 3). This is due to the decreasing concentration of the alkoxide precursor, increasing the intervals among crystals; therefore, this issue would be influential upon the increase of the roughness parameter [8, 10].

Although using PEG causes to form triangular seeds in thin films [12], due to the

low degree of crystallinity and the formation of amorphous thin film, no such particles are observed.

The only effect of PEG is the uniformity and viscosity of the raw film, preventing the formation of any cracks even during the drying and calcining operations.

The quality complimentary inspection of the samples was accompanied by the calculation of R_{Ku} and R_{Sk} values. It is known that if the absolute value of R_{Sk} increases, the quality of coating will not be the same for the whole surface. Therefore, it affects the results obtained from R_{Ku} and correspondingly affects the coating quality based on depths and Kurtosis distribution [21].

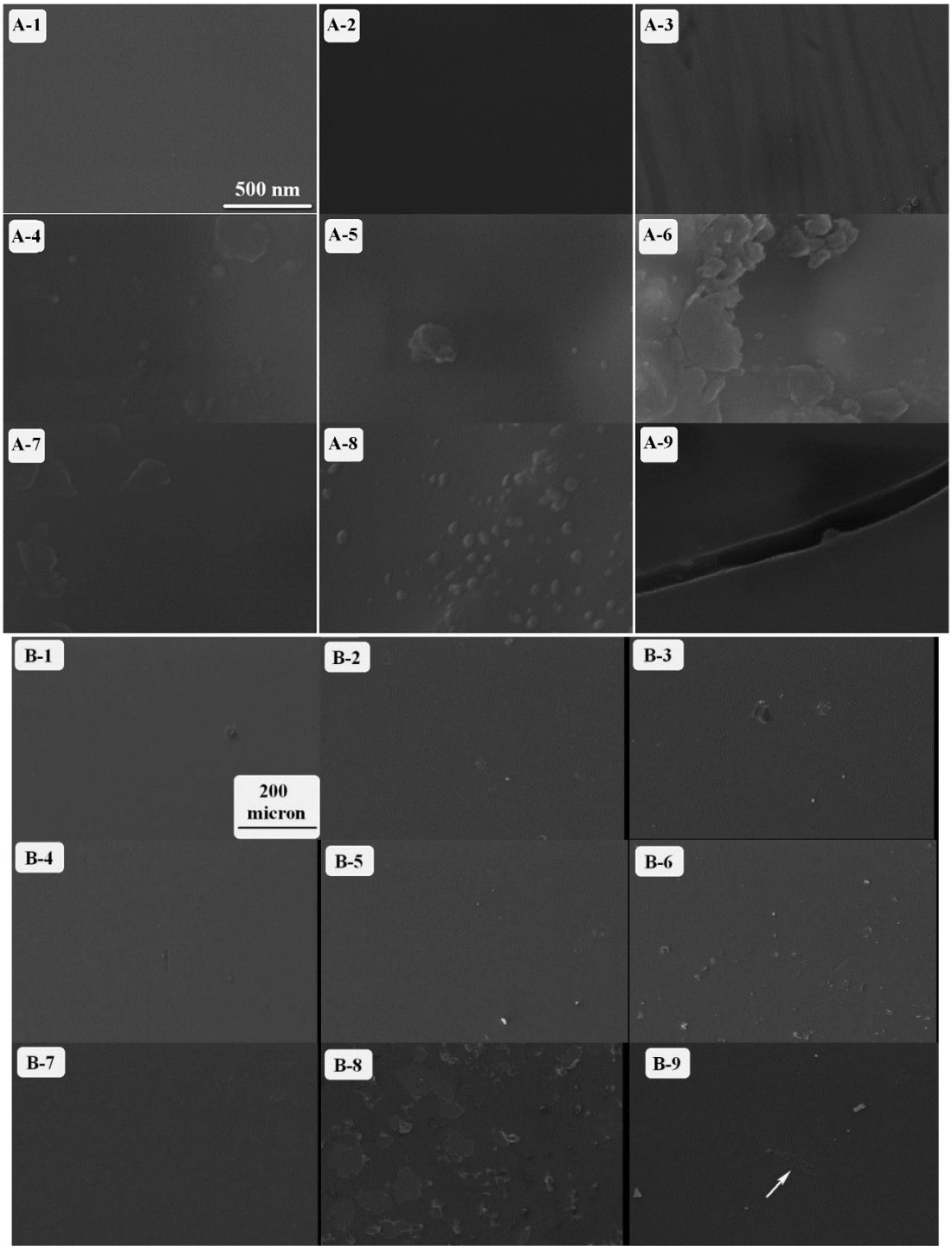

Fig. 2. FESEM images of the coated samples. These figures are related to the samples described in Table 2. (A): at magnifications of 60.000 times. (B): at magnifications of 150 times.

Table 3. The obtained results from AFM analysis of the samples.

Sample	Ra	Rq	Rz	Rq/Ra	Rku	Rsk
1	3.7	4.6	23.2	1.2	3.101	-0.160
2	5.6	25.2	32.4	4.5	31.164	-17.273
3	22.5	28.7	168.2	1.3	3.711	-0.080
4	24.6	39.3	267.6	1.6	9.302	-0.404
5	5.0	7.5	53.1	1.5	8.563	-0.403
6	18.0	24.8	148.0	1.4	7.409	-0.528
7	7.9	18.0	84.3	2.3	75.852	-3.025
8	3.3	6.1	47.7	1.8	31.404	-2.716
9	12.8	21.2	140.5	1.7	20.561	-0.787

Ra: Average roughness, Rq: Root mean square roughness, Rz: Average of five highest peak and five lowest valley, Rq/Ra: Average of root mean square roughness, Rku: Kourtosis roughness, and Rsk: Skewness roughness

3-3-The corrosion behavior of the samples

Fig. 3 indicates Tafel polarization curves of the coated samples compared to the bare sample. Correspondingly, the corrosion parameters are calculated and illustrated in Table 4. The corrosion behavior of the first series of the samples (1, 2, and 3; pH=2) is as follows: by increasing the amount of solvent and calcinations temperature at a constant pH, corrosion current density decreased at first and then increased. On the other hand, in the second series of the samples (4, 5, and 6; pH=4) and also in the third series (7, 8, and 9; pH=6), I_{corr} firstly increases and then reduces in the constant value of pH accompanied by the increase of solvent amount and calcination temperature. It is worth mentioning that the lowest I_{corr} in each set of samples does not yield any meaningful connection to the surface roughness; however, the value changes of R_{Ku} and R_{Sk} are in line with the changes of I_{corr}. In each set of samples, the lowest I_{corr} is observable in which R_{Ku} is regarded as the highest values and R_{Sk} as the lowest values. It should be mentioned that this claim does not apply to the values of R_{Sk} in the second series, maybe due to their close-fit and the increased probability of error in measurements. To elucidate this phenomenon, it should be stated that when the value of R_{Ku} equals 3, a Gaussian distribution and roughness uniformity will be achieved and the surface will be perfectly smooth. However, if the value of R_{Ku} is lower than 3, the stretching of the depths around the average line is higher than that of the heights and if the value of R_{Ku} is higher than 3, accordingly, the stretching of the heights is higher than that of the depths. Also, when the distribution of heights and depths over the surface is symmetrical, then R_{Sk} equals 0; but if the intended distribution is asymmetrical and higher than zero, this shows more distributions of heights compared to depths on the surface and if this amount is less than 0, this shows more distributions of depths compared to the heights [10, 21].

According to the previous research [10], for the first series of the samples, the speed of hydrolysis reaction was higher than the densification reaction rate at pH=2 and upon the increase of the mole ratio of alkoxide to ethanol , the speed of hydrolysis will increase and correspondingly the corrosion rate is reduced. However, upon the temperature increase from 200 to 400 °C, the corrosion speed will increase due to the fast growth of crystallites and the formed changes in the R_{Sk} and R_{Ku} values.

For the second and third series of the samples (keeping away from pH of the isoelectric point), the speed of hydrolysis reaction compared to the first series of the samples is reduced due to the surface charge density. Despite the increase of the solvent amount, the speed of hydrolysis reaction will not overtake compared to the first series of the samples and, consequently, I_{corr} compared to the first series of the samples increases due to the lower amount of crystallites volume per unit. Upon the increase of calcination temperature in the second and third series of the samples, the growth of the particles will take place at the higher speed and the I_{corr} will be reduced.

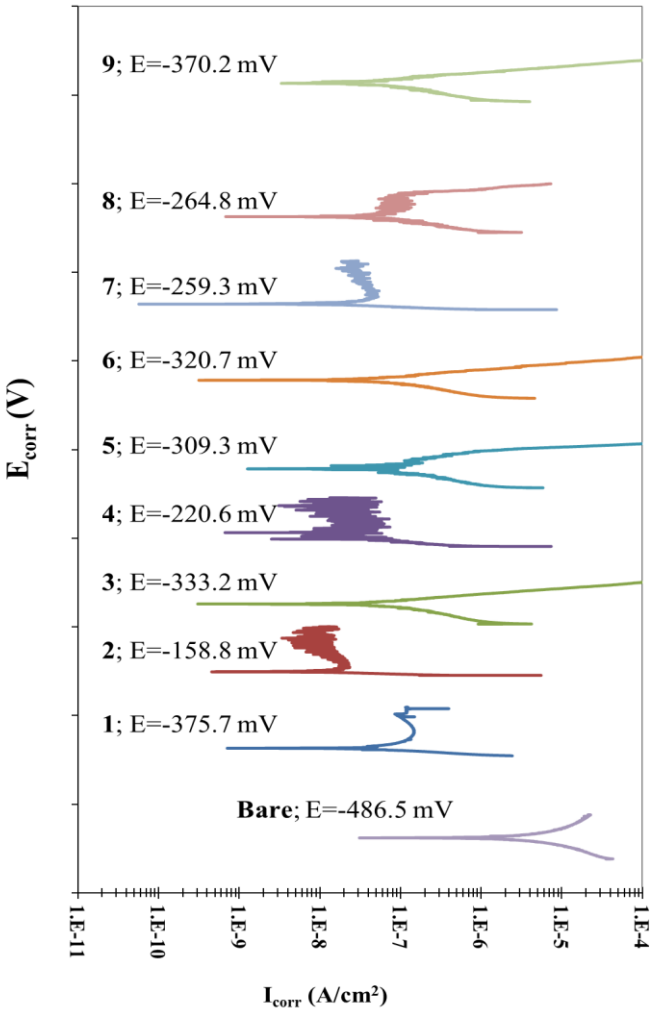

Fig. 3. The Tafel diagrams of the coated samples and the bare steel. To show the behavior of all samples separately in one image, the curves shifted in vertical axis. The actual values of E_{corr} are provided in Table 4.

Table 4. The obtained results from Tafel analysis of the coated samples and the bare sample.

Sample	E_{corr} (mV)	I_{corr} (nA/cm^2)	Ba (mV/dec)	Bc (mV/dec)	Corrosion Protection Efficiency (%) *
1	-375.7	26.98	0.018	-0.013	97
2	-158.8	6.604	0.014	-0.016	99
3	-333.2	17.5	0.02	-0.018	98
4	-220.6	17.44	0.03	-0.04	98
5	-309.3	20.96	0.02	-0.017	97
6	-320.7	17.73	0.04	-0.04	98
7	-259.3	4.068	0.015	-0.009	99
8	-264.8	18.44	0.02	-0.02	98
9	-370.2	13.88	0.03	-0.016	98
Bare Steel	-486.5	855.2	0.014	-0.011	-

* Corrosion Protection Efficiency = [(I_{corr} bare – I_{corr} sample) / I_{corr} bare] * 100

3-4-Samples optimization based on the Taguchi statistical method

The target parameters in this research include roughness and I_{corr}. As it was mentioned before, this research utilized Taguchi statistical method to analyze the obtained results and the optimization of the conditions of the samples as shown in Fig. 4. As can be observed in this figure, pH and temperature have the most effect on I_{corr}. The mole ratio of alkoxide to ethanol is the most effective parameter on R_a. Anyway, based on the intended temperatures of this research, no major changes have occurred in the phase combination, morphology, and the matching of thermal expansion coefficient (between the thin film and the substrate) which

can affect the quality of coating film. According to Fig. 4, it can be predicted that the sample with the specifications of pH=6, the alkoxide to ethanol ratio of 0.167, and the calcination temperature of 300 °C has the lowest I_{corr} and the highest protection performance.

Based on another target parameter (surface roughness), temperature is the most effective one on surface roughness changes, while alkoxide concentration changes do not show any significant impact on this parameter. Thus, the sample with the specifications of pH=6, the alkoxide to ethanol ratio of 0.167 (alkoxide/ethanol=0.167), and the calcination temperature of 200 °C has the lowest roughness. The report by other researchers [22] shows the silica isoelectric point is at pH=2 where the particles are uncharged. This behavior has been observed between the ranges of 1<pH<3 and upon the increase of the pH value, the densification step will be performed at a higher speed compared to the hydrolysis stepdue to the formation of electric charges over the crystallites. Consequently, surface roughness will exceed (the increase of curve slope in pH changes from 2 to 4 as shown in diagram B of Fig. 4), and the more the increase of surface roughness and I_{corr}, the less the protection efficiency of the coatings (indicated in diagram A of Figure 4). Due to the approximation of pH to 7 and the increase of electrical charge of the crystallites surface, and the increase of repulsion among the particles, the growth occurs at higher speed compared to pH=4 and, correspondingly, the surface roughness will be reduced from pH of 4 to 6. In the following, the increase of efficiency of the protection is observable.

According to the obtained results of other researchers [22], when pH and the mole ratio of alkoxide to alcohol are kept constant, consequently, the increase of calcination temperature causes the growth of particles and the increase of the coating surface roughness.
Based on the constant mole ratio of alkoxide to water, upon the increase of the utilized alcohol percentage, the hydrolysis process will be carried out at a higher speed and it shows the reduction of the coating surface roughness due to constant calcination temperature and pH.
The Taguchi results show that the changes of pH and temperature are in line with the roughness changes and corrosion. However, it is the opposite for the ratio changes of alkoxide, i.e. it shows the lowest amount of corrosion on the surface. When pH and the heat treatment are constant, the amount of particles per unit area will increase upon the accretion of the utilized alkoxide amount. Consequently, besides the increase of surface roughness, the reduction of corrosion is observable due to the increase of the coating density [8].

According to the results (Fig. 4), one can express that the optimization values for each sample can be calculated one time through the lowest amount of current corrosion density (LCCD) and another time via the lowest surface roughness (LSR). These values are shown in Table 5. According to the conditions presented in Table 5, both samples to put in the same circumstance were prepared and measured simultaneously.

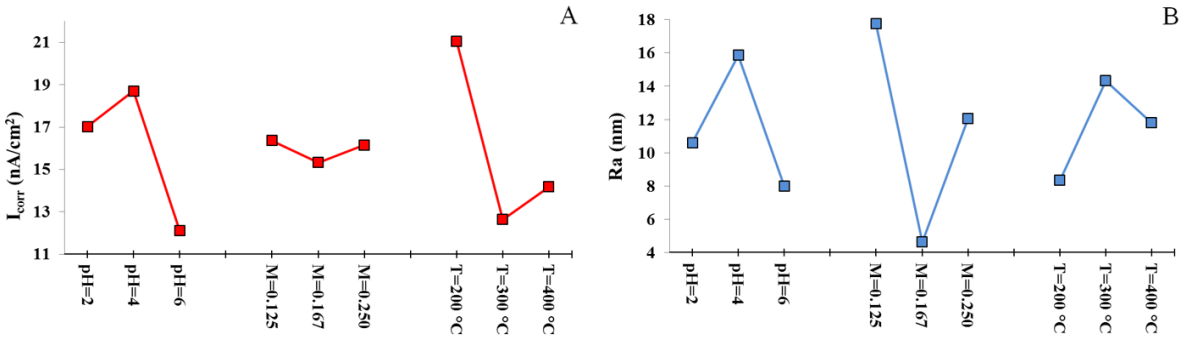

Fig. 4. Mean of mean graphs for I_{corr} and roughness.

Table 5. The optimization condition to maintain the lowest current corrosion density and surface roughness.

Sample	pH of the Sol	Molar Ratio of Alkoxide to Ethanol	Calcination Temperature (ºC)
LCCD	6	0.167	200
LSR	6	0.167	300

The morphology and the coating thickness of the optimized samples are presented in Fig. 5. As can be observed, the samples coatings are uniform and free from cracks. The LCCD coating has 142 μm thickness and the LSR one 333 μm. This increase is due to the higher calcination temperature in the LSR sample causing to increase the number of crystallites and consequently the density of the particles in the thin film. On the other hand, the higher temperature causes to joint crystallites and form thicker film under similar conditions. This thicker film is capable to improve the corrosion behavior. In spite of the fact that film thickness can increase the chance of dissociation, it has a positive effect on the amelioration of corrosion behavior. This issue is consistent with the previously reported results [8].

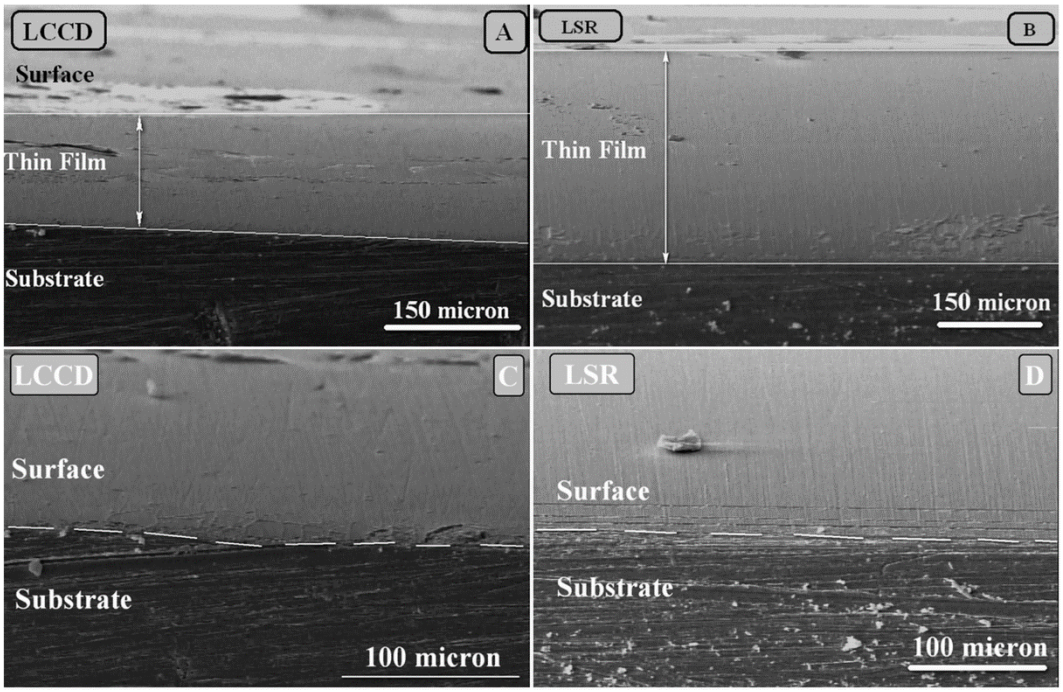

Fig. 5. FESEM images of the LCCD and LSR samples. (A) and (B): The cross-section of the samples at magnifications of 150 times and the determination of the thin film thickness (Thicknesses of LSR and LCCD were measured 333 and 142 μm, respectively). (C) and (D): the surface of LCCD and LSR samples.

AFM parameters of the optimized samples (LCCD and LSR) are presented in Table 6. As can be observed from topography inspection and surface roughness of the samples, the optimized samples have the lowest surface roughness compared to the initial samples (LCCD has the lowest surface roughness). In addition, Tafel diagram and the relevant parameters are presented in Fig. 6 and Table 7, respectively. The results show that the Taguchi method prediction was confirmed due to the determination of the least surface roughness and finally one sample with a roughness of 2.4 nm was obtained. This sample has the highest pH, and the temperature of 200 °C. It seems that 200 °C is appropriate for the formation of uniform thin film. The increase of this temperature to higher values causes to form surface with higher roughness.

I_{corr} of the LCCD and LSR samples was inspected. Importantly, I_{corr} of the LSR sample was measured too low and showed that a sample with good quality of coating was formed in such a way that I_{corr} was consistent with the LCCD sample.

As per the previous study [22], the increase of the utilized solvent amount in the LSR sample compared to LCCD sample, similar pH value, and calcination temperature lead to more hydrolysis of this sample and accordingly the increase of the number of crystallites per unit area comparing to LCCD sample causes the increase of the coating protection efficiency to the amount of 99.7 %.

Fig. 6 shows that I_{corr} of the optimized samples compared to the bare sample has been reduced and the steel passivity over the corrosive environment has been protected.

Consequently, in order to compare and select one of the optimized samples, their abrasion behaviors were inspected through Vickers micro-hardness analysis. Up to now, the LCCD and LSR samples do not show any absolute merit to each other. To introduce the optimized sample, this research scrutinizes the results of surface hardness as illustrated in Table 8. According to these results, LCCD hardness was measured to be higher than that of the reference and LSR samples. Higher hardness depends on the quality of the coating. The only difference between these two samples would be related to the calcination temperature. If the sample has a lower temperature, it has a higher hardness showing its higher density of the particles.

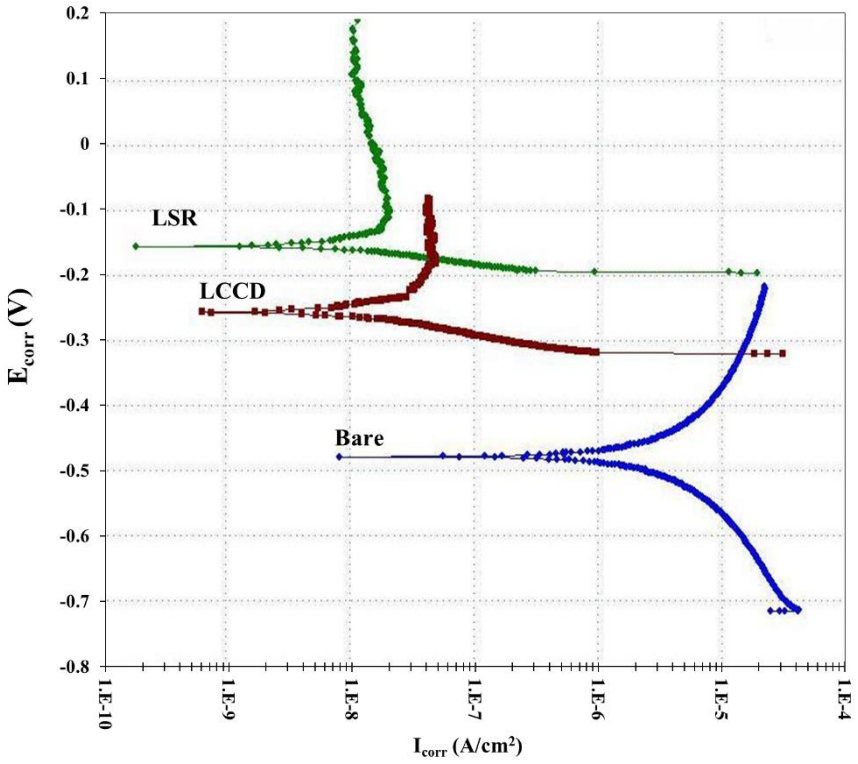

Fig. 6. Tafel diagrams of the optimized samples and the bare steel.

Table 6. The obtained results from AFM analysis of Taguchi samples.

Sample	Ra	Rq	Rz	Rq/Ra	Rku	Rsk
LCCD	2.4	3.6	19.5	1.50	4.33	-0.123
LSR	2.5	3.7	25.2	1.48	5.53	0.060

Table 7. The obtained results from Tafel analysis of Taguchi samples.

Sample	E_{corr} (mV)	I_{corr} (nA/cm^2)	Ba (mV/dec)	Bc (mV/dec)	Efficiency Protection (%)
LCCD	253.8	3.6	0.015	-0.007	99.0
LSR	149.8	2.4	0.017	-0.014	99.7
Bare Steel	-486.5	855.2	0.014	-0.011	-

Table 8. The obtained results from Vickers micro-hardness analysis of Taguchi samples

Sample	Hardness			Average	Standard deviation
LCCD	290	287	297	290	4.39
LSR	220	222	225	222	2.082
Bare Steel	218	219	218	218	0.58

4-Conclusions

The processing of the coated steel was carried out by using amorphous silica to promote corrosion behavior.

The optimization of pH parameters, alkoxide concentration, and calcination temperature was performed through the Taguchi statistical method.

The results obtained from Taguchi analysis showed that pH and the mole ratio of alkoxide to alcohol have the greatest effects on current corrosion density.

The calcination temperature has the most effects on the roughness of the coating surface. Current corrosion density of the optimized sample with surface roughness of 2.5 nm and R_{Ku}= 4.3 was measured as 3.6 A/cm^2, while this amount was 855 A/cm^2 for the bare sample.

The average hardness of the optimized sample was measured to be 290, while this parameter was measured 218 for the reference sample.

References

[1] M. Atik, P. de Lima Neto, L. A. Avaca, M. A. Aegerter and J. Zarzycki, "Protection of 316L stainless steel against corrosion by SiO2 coatings", J. Mater. Sci. Lett., Vol. 13, 1994, pp. 1081-1085.

[2] N. Birks, G. H. Meier and F. S. Pettit, Introduction to the High Temperature Oxidation of Metals, 2nd ed., Cambridge University Press, University of Pittsburgh,
2006.

[3] G. Y. Lai, High-Temperature Corrosion and Materials Applications, ASM International, 2007

[4] Y. S. MHAISAGAR, B. N. JOSHI and A. M. MAHAJAN, "Surface texture modification of spin-coated SiO2 xerogel thin films by TMCS silylation", B. Mater. Sci., Vol. 35, 2012, pp. 151-155.

[5] G. Carbajal-de la Torre, M. A. Espinosa-Medina, A. Martinez-Villafañe, J. G. Gonzalez-Rodriguez and V. M. Castaño, "Study of Ceramic and Hybrid Coatings Produced by the Sol-Gel Method for Corrosion Protection ", Open Corr. J., Vol. 2, 2009, pp. 197-203.

[6] P. Sangpour, K. Khosravy and M. Kazemzad, "Investigation of SiO2 thin films dielectric constant using ellipsometry technique", Iran. J. Phys. Research, Vol. 14, 2014, pp. 161-166.

[7] C. J. Brinker and G. W. Scherer, Sol-Gel Science: The Physics and Chemistry of Sol-Gel Processing, 1st ed., Elsevier Science, Academic press, 2013.

[8] T. P. Chou, C. Chandrasekaran, S. Limmer, C. Nguyen and G. Z. Cao, "Organic-inorganic sol-gel coating for corrosion protection of stainless steel", J. Mater. Sci. Lett., Vol. 21, 2002, pp. 251-255.

[9] D. A. López, N. C. Rosero-Navarro, J. Ballarre, A. Durán, M. Aparicio and S. Ceré, "Multilayer silica-methacrylate hybrid coatings prepared by sol–gel on stainless steel 316L: Electrochemical evaluation", Sur. Coat. Tech., Vol. 202, 2008, pp. 2194-2201.

[10] M. Houmard, E. H. M. Nunes, D. C. L. Vasconcelos, G. Berthomé, J. C. Joud, M. Langlet and W. L. Vasconcelos, "Correlation between sol–gel reactivity and wettability of silica films deposited on stainless steel", Appl. Surf. Sci., Vol. 289, 2014, pp. 218-223.

[11] L. L. Hench, D. R. Ulrich, U. o. F. D. o. M. Science, Engineering and U. o. F. C. o. Engineering, Ultrastructure processing of ceramics, glasses, and composites, Wiley, New York, 1984.

[12] S. Naghibi, S. Vahed, O. Torabi, A. Jamshidi and M. H. Golabgir, "Exploring a new phenomenon in the bactericidal response of TiO2 thin films by Fe doping: Exerting the antimicrobial activity even after stoppage of illumination", Appl. Sur. Sci., Vol. 327, 2015, pp. 371-378.

[13] A. Jamshidi, A. A. Nourbakhsh, S. Naghibi and K. J. D. MacKenzie, "Application of the statistical Taguchi method to optimize X-SiAlON and mullite formation in composite powders prepared by the SRN process", Ceram. Inter., Vol. 40, 2014, pp. 263-271.

[14] H. Hasannejad, M. Aliofkhazraei, A. Shanaghi, T. Shahrabi and A. R. Sabour, "Nanostructural and electrochemical characteristics of cerium oxide thin films deposited on AA5083-H321 aluminum alloy substrates by dip immersion and sol–gel methods", Thin Solid Films, Vol. 517, 2009, pp.

4792-4799.
[15] A. Ghasemi, T. Shahrabi, A. A. Oskuie, R. K. Roy, A Primer on the Taguchi Method, Society of Manufacturing Engineers, 2nd ed., SME, 1990.
[16] M. Raposo, Q. Ferreira and P. A. Ribeiro, "A guide for atomic force microscopy analysis of soft-condensed matter", Mod. resear. edu. topics microscopy, Vol. 1, 2007, pp. 758-769.
[17] A. Phanasgaonkar and V. S. Raja, "Influence of curing temperature, silica nanoparticles- and cerium on surface morphology and corrosion behaviour of hybrid silane coatings on mild steel", Sur. Coat. Tech., Vol. 203, 2009, pp. 2260-2271.
[18] H. Hasannejad and S. Sanjabi, "Effect of heat treatment on corrosion properties of sol–gel titania–ceria nanocomposite coating", J. Alloy. Comp., Vol. 504, 2010, pp. 237-242.
[19] P. Sarah, K. Venkateswarlu, B. W. Shivaraj, H. N. N. Murthy, M. Krishna and B. S. Satyanarayana, "Effect of Annealing Temperature on Structural and Optical Properties of Dip and Spin coated ZnO Thin Films", 2nd International Conference on Nanomaterials and Technologies, Procedia Materials Science, 2015, p. 292.
[20] S. Naghibi, A. Jamshidi, O. Torabi and R. E. Kahrizsangi, "Application of Taguchi Method for Characterization of Corrosion Behavior of TiO2 Coating Prepared by Sol-Gel Dipping Technique", .Appl. Ceram. Tech., Vol. 11, 2014, pp. 901-910.